Iron geochemistry in a contaminated urban soil dedicated to stormwater infiltration

Qiufang Zhan[1], Vincent Chatain[1], Mathieu Gautier[1], Clémentine Drapeau[2], Mostafa Benzaazoua[1,3], Hassan Bouzahzah[4] , Laurent Lassabatère[2], Gislain Lipeme Kouyi[1], Cécile Delolme[1]

[1] Univ Lyon, INSA Lyon, DEEP (Déchets Eaux Environnement Pollutions), EA 7429, 69621 Villeurbanne Cedex, France

[2] Univ Lyon, LEHNA (Laboratoire d'Ecologie des Hydrosystèmes Naturels et Anthropisés), CNRS, UMR 5023, ENTPE, Vaulx-en-Velin, 69518, France

[3] UQAT-Polytechnique, IRME (Institut de Recherche en Mines et Environnement (IRME), 445 Boul. de l'Université, Rouyn-Noranda, J9X 5E4, Canada

[4] Université de Liège (ULG), Laboratoire de Génie Minéral, Matériaux et Environnement (GeMMe). Allée de la découverte, 13/A. Bât. B52/3 Sart-Tilman. 4000 Liège, Belgique.

Keywords

Urban sediments, Iron, Speciation, Trace Metals, Sequential Extraction, Sediment Management, Environmental Assessments

Abstract

In urban areas, stormwater infiltration basins considerably trap suspended solids, which form a surface soil (sedimentary layer) with high metals and organic compounds contents. Among metals, Fe is a key parameter, which is one of the dominant redox-active elements in this soil and which affects a wide range of processes; including biogeochemical cycling, toxicity and bioavailability of trace contaminants.

This study considers the spatial variability of major and trace elements (Fe in particular) from a surface soil in Django Reinhart stormwater infiltration basin (Chassieu, eastern suburbs of Lyon, France), their speciation and their potential reactivity characterization.

The sediments collected in three different zones (dry, wet, saturated) were mainly analyzed through partitioning of iron (sequential extraction), mineralogical and infrared spectroscopy observation. The elements speciation appears to be roughly homogenous, including the particle size, the total content and the mineral phases which are typically alumino-silicates with high contents of Si, Al and Fe and the sediments are highly organic (18 - 27 wt.%). Few differences in Fe portioning were spatially observed. Results demonstrated that acid soluble Fe (18 - 23 wt.%), crystalline oxides Fe (28 - 30 wt.%) and residual Fe (40 - 45 wt.%) constitute the main part of the total Fe. Fe bound to silicate is residing in this residual fraction. On the contrary, exchangeable Fe, organic-bound Fe and pyrite-bound Fe involve small parts. The low content of Fe bound to pyrite is probably due to oxic conditions. This study provides not only a basis for the rational interpretation of Fe partitioning and speciation in urban sediments, but also provides important features regarding their management.

Introduction

The urban environment will soon become the most dominant human habitat in history. The pressure from the activities of the urban population is intense, as anthropogenic emissions of potentially profound health implications of toxic trace metals have accelerated considerably [1]. In urban environments, infiltration of stormwater and runoff water is a management mode which is considerably developing in order to recharge groundwater aquifers,

to protect from flooding and to limit the direct release of those effluents in surface receiving environment [2]. Thus, stormwater infiltration systems concentrate, on ground surfaces of a few hectares, the supply of urban catchment basin rainwater. Suspended matter carried on by the rainwater, accumulate on the surface and lead to the formation of a sedimentary layer which is very organic and can be highly contaminated (trace metals, aliphatic and aromatic hydrocarbons, pesticides, PCB, etc.) [2–4] . These materials are composed of a complex mixture of natural and manufactured solid particles from the nanometric to the centimetric scale. These layers play a major role in urban environmental biogeochemical cycles of major and trace elements. The environmental risk linked to the presence of these polluted layers in urban environment need to be better described and studied. It is consequently essential to carry out a continuous effort for the production of new knowledges on these specific interfaces and improve their management.

The majority of the research works dedicated to urban stormwater sediments characterization have been focused on heavy metal contents (Zn, Cu, Ni, Pb, Cr, etc.) assessment [5, 6] or on their speciation and potential mobility evaluation [3, 6, 7].

Despite these numerous studies, it is still impossible to understand and predict the evolution and reactivity of these sediments depending on different environmental conditions. We assume that it is necessary to include multi-element studies to understand elemental cycles in urban interfaces [11–13]. In the context of urban sediments, very few studies were dedicated to multi element studies coupling major and trace mineral and reactivity characterization. Several studies [11-14] highlighted the key role of iron in natural environments. Despite iron (Fe) was found in non-negligible concentration in urban sediments (from 2.52 to 3.92 wt. %), to our knowledge the only data available on Fe speciation were produced by Clozel et al. (2006). Scanning electron microscope (SEM) observations of samples from three different urban stormwater sediments coupled with Energy Dispersive Spectroscopy distinguished spheroid of Fe^0, different types of Fe oxi-hydroxides sometimes associated with traces of Ti, Zn, Cu, alloys fragments containing Fe and Cr and glass fragments with Si, Fe, Al, Ca.

It is well known that Fe is intimately involved in the geochemistry of sediments essentially through the redox couple Fe(II)/Fe(III) that is of major importance to a number of major or trace elements cycling processes [12]. Fe(III)- oxi-hydroxides are particularly effective, sorbents of metal cations and oxyanions [15–18] because of their small particle size (i.e., high surface areas), in the case of cations, their relatively high pH value at the point of zero charge [19, 20], thus favoring a negative electric charge under environmental pH, and cation exchange capacity.

In this context, the main objective of the study was to focus on the speciation and the potential mobilization of Fe and related heavy metals in urban stormwater sediments accumulated at the surface of an infiltration basin. Through an experimental approach, based on multidisciplinary investigations [21–24], the spatial and temporal evolution of the content and speciation of Fe was investigated and related to the functioning of the basin.

Materials and methods

Materials and experimental site

The infiltration basin studied is located at Chassieu, an urban area NE of Lyon, France. The one ha infiltration basin receives stormwater from an urban and industrialized watershed of 185 ha and was described previously [23]. The sampling area is located in the infiltration basin where sediments have accumulated since 2004.

In order to see the influence of the water saturation degree on iron speciation, sediments were collected in three different areas (Fig.1) in July 2013. The first area is located at the basin entry which is always submerged by the water. The 25 cm thick layer of sediment was colonized by aquatic vegetation. This zone is named "Saturated zone". The second area called "Wet zone" corresponds to a frequently immerged zone. The third one is located in a "Dry zone" where sediments have been accumulated during 6 months between November 2012 and March 2013 due to a direct discharge of stormwater through a bypass near this zone.

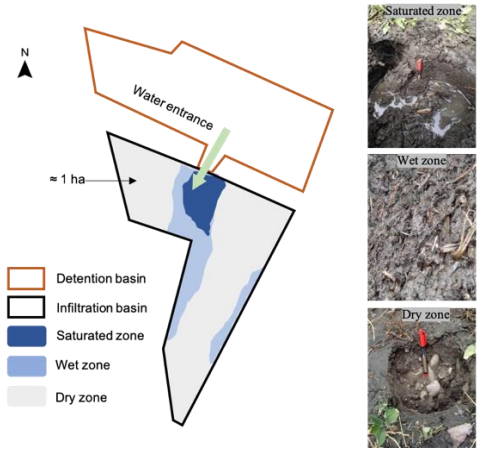

Fig. 1: Location of the 3 areas sampled in the infiltration basin

For each zone, a representative sample of 3 to 5 kg of sediment was constituted from three different collected samples. They were homogenized and passed through a 4-mm sieve at the laboratory and immediately frozen, lyophilized and kept at 4°C before analysis.

Analytical methods

Chemical characterization

The sediments were characterized for pH, particle size distribution (PSD), chemical composition and total organic carbon (TOC). Analyses for pH is performed at laboratory according to French standard methods [39]. Moisture content is typically measured by oven-drying approximately 24 h at 105°C. PSD was determined by laser diffraction (Malvern Mastersizer 2000G) after sieving the sediment at 1mm. Total carbon content was determined by induction furnace analyzer (ELTRA CS-2000). Chemical composition was determined by inductively coupled plasma atomic emission spectroscopy (ICP-AES, Perkin Elmer Optima 3100 RL) after a $HNO_3/Br_2/HF/HCl$ digestion. Content in organic matter (OM) was determined by TOC through sample combustion within a furnace heated to 500°C. The released gas was then analyzed with non-dispersive infrared gas apparatus.

Mineralogical characterization

X-ray diffraction

The mineralogy of samples was determined by X-ray diffraction (XRD) (Bruker AXS D8 advance) equipped with a copper anticathode, scanning over a diffraction angle (2θ) range from 5° to 70°. Scan settings were 0.02° 2θ step size and 4s counting time per step. The DiffracPlus EVA software (v.9.0 rel.2003) was used to identify mineral species and the TOPAS software (v 2.1) implementing Rietveld refinement was used to quantify the abundance of all identified mineral species [24]. The absolute precision of this quantification method is of the order of ±0.5-1wt.%.

Optical microscopy and scanning electron microscopy

The samples mineralogy identification was completed by optical microscopy observations. Polished sections prepared with bulk samples (sediment impregnated within an Epoxy resin) were observed by reflected light microscopy (Zeiss Axio Imager.M2m). The chemical composition of the individual minerals (stoichiometry) was determined using a scanning electron microscope (Hitachi S-3500N) equipped with an Energy Dispersive Spectrometer (EDS, Silicon Drift Detector X-Max 20 mm², Oxford) operated under the INCA software (450 Energy). The operating conditions were 20kV, ~100 µA and 15 mm working distance.

The Fourier transform infrared spectroscopy (FTIR)

The Fourier transform infrared spectroscopy (FTIR) measurements were performed using a Bruker AXS Model IFS 55 equipped with a broadband (6000-600 cm^{-1}) mercury-cadmium telluride detector and cooled with liquid nitrogen. FTIR contains relevant information on the molecular composition of inorganic and organic matter, which is a promising tool for the quantitative assessment of minerals, organic functional groups, protein structures and tissues. The FTIR measurements were performed on grinded sediment samples for compounds identification.

Sequential chemical extraction

In order to understand the operational fractionation (speciation) of iron in the surface sediments of the Django Reinhardt infiltration basin, a sequential chemical extraction procedure adapted from Claff et al. (2010) was carried out in triplicate. The objective was to determine the distribution of six fractions: defined operationally, namely exchangeable Fe, acid soluble Fe, organic Fe, crystalline Fe oxides, Fe in pyrite and residual Fe, for the constituents of interest in the sediment. The following six fractions were examined as showed in Fig.2:

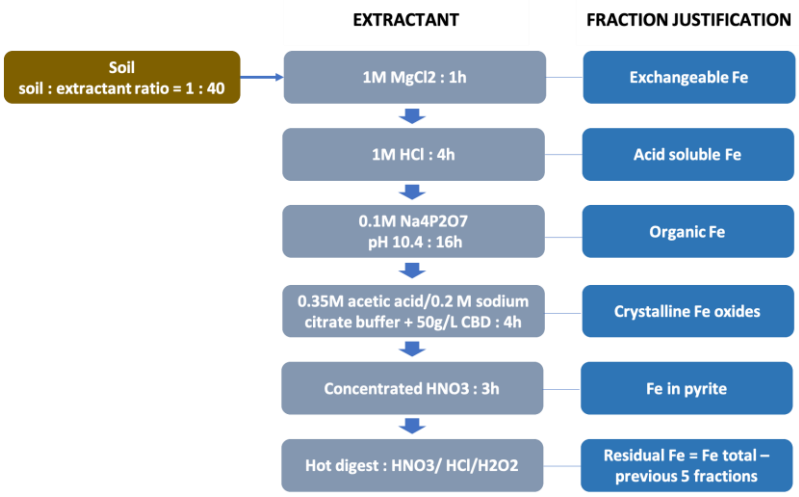

Fig. 2: Sequential extraction procedure adapted from Claff et al. (2010)

To carry out the experiments, 1 g of dry lyophilized sediment is weighed into a 40 ml polyethylene centrifuge tube to which the sequential extraction protocol described in Fig.2 is applied. The dry sediment / extractant ratio for the first 5 steps is 1g DM / 40ml. between two successive extraction steps, the sediment is centrifuged for 20 minutes at 4000 rpm. The supernatant is then filtered (0.45 µm filter) and acidified if necessary with a few drops of nitric acid and iron was then analyzed by ICP-AES. The filtrates are stored at 4° C in polyethylene bottles before analysis. The remaining solid is used for the following characterization steps after washing with demineralized water (10 ml), centrifugation and filtration.

Results

The water content, OM content, major element content and particle size distribution of the sediments in the three sampled zones are summarized in Table 1. The sediment particle size of the fraction < 1mm is not homogeneous throughout the basin, a decrease in particle size is noted from the dry zone to the saturated one. The dry zone has received raw stormwater before the sampling period leading to erosion that may explain the change in particle size spatial distribution. The organic matter content is ranging from 17.5 wt.% to 26.8 wt.%, which is higher than the values classically reported for soils (0.93 wt.% to 4.5 wt.%) [26–28]. The high level of organic matter can be explained by the accumulation of fine natural organic particles and hydrocarbon particles [2] carried on by stormwater and deposited on the basin. In addition, the presence of vegetation on the surface also contributes to the increase of organic matter content. The samples in the 3 zones have similar total element contents, with contents of Si, Al and Fe, ranging from 20 to 24 wt.%, 3.3 to 5.2 wt.%, and 2.7 to 3.9 wt.%, respectively. The main source of Si and Ca (up to 6.2 wt.%), generally the most abundant element of the earth's crust, is probably the minerals of the soil that were weathered and leached by stormwater and its own texture [28]. In these sediments, Ca is mainly in the carbonate form like calcite, as revealed by X-ray diffraction (Table 2). Phosphorus (P) content varies from 0.13 wt.% to 0.24 wt.%, meaning that urban sediments can be seen as good P sinks, the wet zone and saturated zone have the similar content and the dry zone has the minimum content. It could be explained by the presence of vegetation preferentially in the wet and saturated zones which can be rich in organic-bound phosphorus. The homogenous sulfur content could be linked to the content of pyrite (Table 2). The trace metals concentration range from 1655 to 2294 ppm for Zn, 223 to 286 ppm for Cu, 178 to 242 ppm for Cr, 163 to 269 ppm for Pb, 79 to 121 ppm for Ni. The concentrations of these five metals is above the thresholds (NOR: DEVO0650505A - Decree of 9 August 2006 concerning the levels to be taken into account for valorization of basin sediment in France) [40] and then could be considered as a potential source of pollution in terms of risk assessment.

Table 1 : Physicochemical characterization of the sediment

Characteristic	Dry zone	Wet zone	Saturated zone	*Thresholds (NOR: DEVO0650505A)*
Granulometry	Texture: Loam D10: 6.64 µm D50: 59.93 µm D90: 506.85 µm	Texture: Silt loam D10: 3.11 µm D50: 22.32 µm D90: 187.39 µm	Texture: Silt loam D10: 3.33 µm D50: 20.38 µm D90: 125.46 µm	-
pH	7.0	7.0	7.0	-
Water content (wt.%)	20.9±0.8	52.6±4.6	66.5±0.6	-
Organic matter (wt.%)	17.5	26.8	22.2	-
Si (wt.%)	23.97	20.95	20.13	-
Ca (wt.%)	6.21	1.96	5.43	-
Al (wt.%)	3.23	5.17	4.24	-
Fe (wt.%)	2.69	3.91	3.29	-
P (wt.%)	0.13	0.24	0.23	-
S (wt.%)	0.22	0.29	0.22	-
Zn (ppm)	1655	2294	1873	*300*
Cu (ppm)	223	237	286	*100*

Cr (ppm)	242	193	178	*150*
Pb (ppm)	177	269	163	*100*
Ni (ppm)	112	121	79	*50*

The sediments sampled from the 3 zones have the similar mineral phases (Table 2). They are mainly composed of quartz, illite and calcite. In addition, a small amount of rutile and magnetite, as well as pyrite were observed in these 3 sediments, with less than 0.5 wt.%. The high calcite contents is directly associated to the calcareous subsoil characteristic as mentioned previously. The contents of chlorite and illite show the same tendency: dry zone < saturated zone < wet zone. The few content of chlorite and illite in the sediment of the dry zone can be explained by the seasonal change of stormwater quality arriving in the basin (sometimes without arrivals in dry zone) and the draining of the dry zone during the winter. The absence of calcite in wet zone is probably due to the leaching in this zone with the circulation of water. In addition, the distance from the entry may have conditioned different pattern in terms of sediment deposition.

Table 2: Mineral phase's characterization and contents (% of dry mass)

Mineral phase	Formula	Dry zone (wt.%)	Wet zone (wt.%)	Saturated zone (wt.%)
Quartz	SiO_2	32.0	22.4	21.3
Calcite	$CaCO_3$	14.1	4.6	12.4
Illite	$K_{0.65}Al_{2.0}[Al_{0.65}Si_{3.35}O_{10}](OH)_2$	10.0	22.0	14.0
Chlorite	$[(Mg,Fe,Ni,Mn)_5Al](AlSi_3)O_{10}(OH)_8$	4.8	11.0	9.0
Plagioclase	$NaAlSi_3O_8 - CaAl_2Si_2O_8$	7.5	6.6	6.8
Orthoclase	$K(AlSi_3O_8)$	3.4	0	4.3
Hornblende	$(Ca,Na,K)_2(Mg,Fe^{2+},Fe^{3+},Al)_5$ [Si6(Al,Si)2O22](OH,F)2	5.0	0.7	1.1
Pyrite	FeS_2	0.4	0.5	0.4
Rutile	TiO_2	0.4	0.5	0.4
Magnetite	$Fe^{2+}Fe^{3+}{}_2O_4$	0	0.1	0.1

Optical and Scanning Electron Microscopic observations were performed to describe mineral and trace element-bearing phases (Fig. 3). SEM analyses pointed out the occurrence of micrometric pyrite (around 10 to 15 µm, Fig. 3). Its mass percentage was calculated on the basis of the sulfur content in the sample (element to mineral conversion). Some pyrites showed a minor replacement into pyrrhotite.

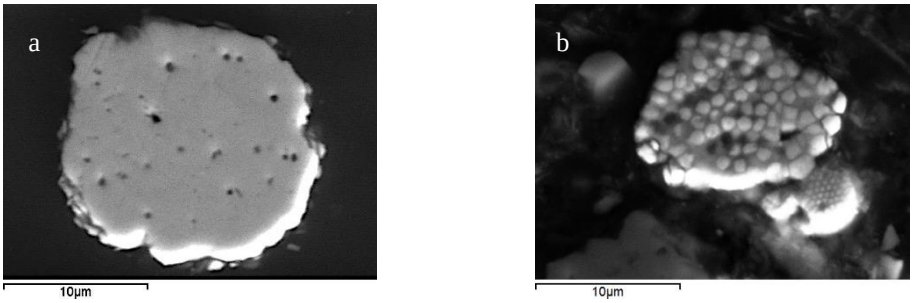

Fig. 3 : SEM microscopy images (a) and (b) showing minerals pyrite and framboid pyrite in the wet zone

In general, the similar spectra indicates that the composition of these three samples is very close (Fig.4). The sediment spectra can be divided into few main regions. The broad absorption bonds between 3400 cm^{-1} and 3620 cm^{-1} were dominated by O-H stretching vibrations of the organic matter and clay minerals. The 2860–2930 cm^{-1} range was primarily responsible for C-H of the sediment organic matter. The peaks at approximately 1874 cm^{-1} and 1797 cm^{-1} respectively indicate the presence of quartz. The intensity of bond at around 1645 cm^{-1} was assigned to C=C bending in aromatic cycles. More pronounced difference related to the vibration of $CaCO_3$ at 1451 cm^{-1} was observed for the wet zone, in accordance with the observations of the mineral phases in Table 2 (14.1wt.% and 12.4wt.% by mass in the dry zone and saturated zone, only 4.6wt.% for the wet zone).

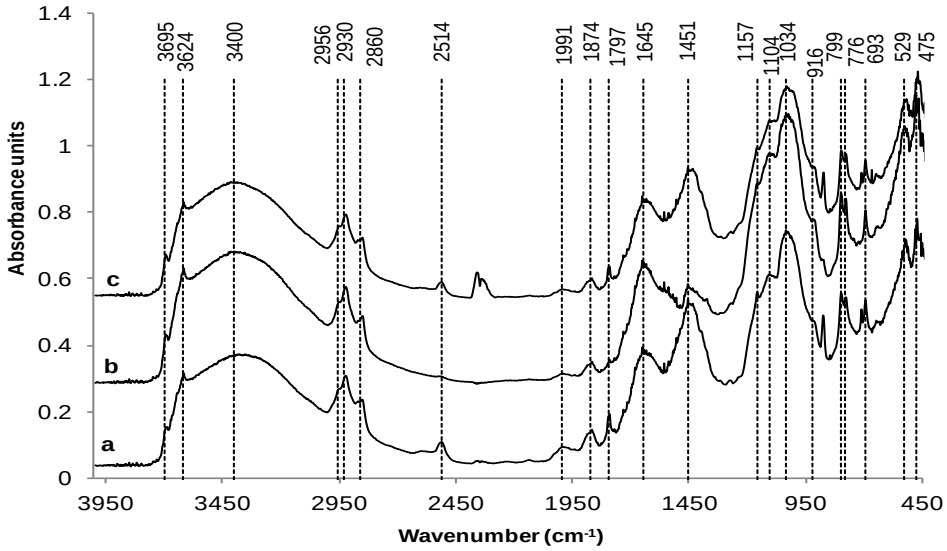

Fig. 4 : Typical FT-IR spectra of sediment: dry zone (a), wet zone (b), saturated zone (c)

The results obtained for the triplicates through the Fe sequential extraction shows less than 5% of variability, allowing the presentation of the arithmetic average of the three values for each fraction. The Fe speciation specified through the sequential extraction procedure of Claff et al. (2010) is shown in Fig.5.

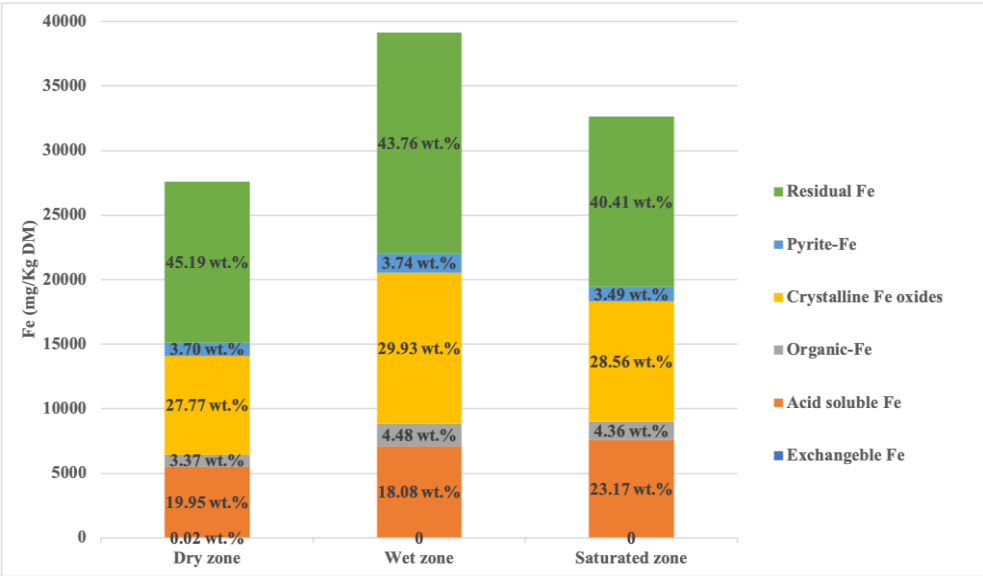

Fig. 5: Fe content in the sequential extraction phases adapted with the Claff et al. (2010) method

Results indicate a very low Fe content in the exchangeable fraction ($MgCl_2$ extraction) (<0.02 wt.%) for the 3 samples. This observation coheres the results obtained (<1wt.%) by Claff et al. (2010). The acido-soluble Fe is much higher with contents ranging from 18.1 wt.% to 23.2 wt.%. This phase corresponds to the solubilization all the minerals sensitive to low pH, including carbonates and poorly ordered sulfides and oxides. The organic-bound iron fraction is quite low (approximately 4 wt.%). The fourth extraction step represents crystalline iron oxides and corresponds to nearly 30 wt.% of the total Fe. The pyrite-bound iron extracted by HNO_3 appears to be very stable depending on the sampling zones (3.74 wt.% to 3.49 wt.%). The residual iron content obtained by subtracting the sum of iron extracted from the first 5 steps to the total iron sediment content, is high with contents ranging from 40.41 wt.% to 45.19 wt.% for the 3 samples.

Compared to Claff et al. (2010), citrate buffered dithionite (CBD)-extractable Fe is much higher in our sediments (40 wt.% versus ~5 wt.%). CBD is a strong reducing agent and widely used to extract both the poorly ordered and crystalline iron oxide fraction, such as ferrihydrite, goethite and hematite [28]. The enrichment of Fe in oxidized layer may have been caused by periodic freshwater flooding and redox cycling. Dissolved Fe^{2+}, produced by the reductive dissolution of Fe minerals during freshwater flooding, could be transported by diffusion to the upper oxidized layer and also by leached from the overlying topsoil [31, 32]. Dissolved ferrous iron may have moved upward via evaporation transport during dry conditions to oxidize and to form Fe(hydr)oxides such as schwertmannite, ferrihydrite, lepidocrocite, jarosite, natrojarosite, goethite, and hematite [32]. These results indicate for 3 sediment samples where iron oxide contents (from 27.77 wt.% to 29.93 wt.%) are very high, but the CBD extraction step is not able to completely dissolve crystalline iron oxide minerals, especially goethite, hematite and other crystalline minerals. It means that the crystalline iron oxides remains in the residual fraction of the sequential extraction procedure [32]. Thus, the major form of Fe in the sediment was crystalline oxide minerals. The proportion of pyrite-bound Fe was low in comparison the results of Claff et al. (2010), when comparing the sediment sampled at depths 2.0-2.2m, whereas it was similar for the surface layer (0.49-0.52m). These results are in good agreement with those of Huang et al. (2017) (acid sulfate paddy soils) and Sukitprapanon et al. (2018) (acid sulfate soil), who have also indicated that the proportion of pyrite-bound Fe was lower in the partially oxidized zone.

The total Fe content in the studied basin, 25.69 mg/g Dry Matter, is very similar to the average total Fe content in sediments collected in others stormwater infiltration basins in French industrial watersheds (25.80 mg/g DM, Table 3).

Table 3 : Total iron content in different type of sediments collected in different context

Resource	Name	Sediment collection context	Country	Fe (mg/g DM)	Mean Fe (mg/g DM)
Winiarski (2014)	Leopha	stormwater infiltration basin in industrial watersheds	France	25.68	25.80
	Minerve		France	29.51	
	PAE Mi-plaine		France	35.39	
	Charbonnier		France	18.25	
	D, Reinhardt		France	25.69	
	IUT DOUA		France	20.49	
	ZAC des Pivolles		France	13.36	
	ZAC du Chêne		France	30.55	
	ZAC Pesseliere		France	33.29	

	Chemin de Feyzin	stormwater infiltration basin in agricultural watersheds	France	13.78	20.43
	Grange Blanche		France	25.42	
	Parilly		France	18.64	
	Pierre Blanche		France	23.34	
	Villardier		France	20.97	
Couvidat et al.(2018)	Mediterranean harbor	marine	France	34.00	31.57
E. Agarry and N. Owabor (2011)	Rivers State		Nigeria	20.20	
Sáez et al.(2003)	Bay of Cádiz		Spain	40.50	

On the other hand, the iron content of the sediment basin is higher than the average iron content for agricultural watershed (20.43 mg/g DM) and lower than that for marine sediments (31.57 mg/g DM). The comparison of total iron content among industrial drained basin sediments, drained marine sediments and agricultural basin sediments not only shows the iron content in environmental context but also gives the information that iron is fairly concentrated in urban basin sediments.

Conclusions

This study highlights the significant amount of Fe found in the sediment of urban stormwater infiltration basin, probably because Fe being a key energy source for microbes, the redox cycling of Fe is intimately linked to other elemental cycles. Indeed the reduction of Fe(III) is often tied to the oxidation of sulfur (from sulfide to sulfate) [11], this process can act as long-term sinks for contaminant metals. In the studied sediments, approximately 20 wt.% of total Fe was HCl-extractable Fe. This fraction can be related in this case to carbonates, oxides and poorly ordered sulfides, which could be linked to Fe redox transformation, *i.e.* pyrite oxidation under oxic conditions.

The Fe sequential extraction proposed by Claff et al. (2010) was dedicated to acid sulfate soils, whereas the studied sediment are carbonated neutral materials. Whilst results of this study provide a basis for the rational interpretation of iron partitioning in the urban sediment via this sequential extraction procedure. In addition, this study highlights the need to optimize the quantity of iron mineral analyzed as CBD is not able to completely dissolve crystalline iron oxide minerals, *e.g.* the minerals in the residual Fe fraction. Iron minerals are not only under crystalline forms but also exist in amorphous Fe, and a part of them are reducible.

On the other hand, this study aims to combine other sequential extraction methods (such as Van Bodegom et al. 2002) to better understand the key factor that controls Fe speciation, its role in sediment oxidation-reduction process and the potential mobilization of iron and heavy metals. These are valuable information for the urban sediments management, environmental assessments and in the stormwater infiltration organization.

Acknowledgements

The authors are grateful to CNRS EC2CO and BQR INSA Lyon for their logistic and financial support and Tiphaine Legendre for her precious help in the experiments.

References

[1] C. S. C. Wong, X. Li, and I. Thornton, "Urban environmental geochemistry of trace metals," *Environmental Pollution*, vol. 142, no. 1, pp. 1–16, Jul. 2006.

[2] B. Chocat, *Encyclopédie de l'hydrologie urbaine et de l'assainissement*. Paris: Technique & Documentation-Lavoisier, 1997.

[3] A.-L. Badin, J.-P. Bedell, and C. Delolme, "Effect of water content on aggregation and contaminant leaching: the study of an urban Technosol," *Journal of Soils and Sediments*, vol. 9, no. 6, pp. 653–663, Dec. 2009.

[4] A. El-Mufleh Al Husseini, B. Béchet, A. Gaudin, and V. Ruban, "Trace metal fractionation as a mean to improve on the management of contaminated sediments from runoff water in infiltration basins," *Environmental Technology*, vol. 34, no. 10, pp. 1255–1266, May 2013.

[5] M. C. Kondo, R. Sharma, A. F. Plante, Y. Yang, and I. Burstyn, "Elemental Concentrations in Urban Green Stormwater Infrastructure Soils," *Journal of Environment Quality*, vol. 45, no. 1, p. 107, 2016.

[6] T. Winiarski, J.-P. Bedell, C. Delolme, and Y. Perrodin, "The impact of stormwater on a soil profile in an infiltration basin," *Hydrogeology Journal*, vol. 14, no. 7, pp. 1244–1251, Nov. 2006.

[7] B. Clozel, V. Ruban, C. Durand, and P. Conil, "Origin and mobility of heavy metals in contaminated sediments from retention and infiltration ponds," *Applied Geochemistry*, vol. 21, no. 10, pp. 1781–1798, Oct. 2006.

[8] M. Saulais, J. P. Bedell, and C. Delolme, "Cd, Cu and Zn mobility in contaminated sediments from an infiltration basin colonized by wild plants: the case of Phalaris arundinacea and Typha latifolia," *Water Sci. Technol.*, vol. 64, no. 1, pp. 255–262, 2011.

[9] J. Kaye, P. Groffman, N. Grimm, L. Baker, and R. Pouyat, "A distinct urban biogeochemistry?," *Trends in Ecology & Evolution*, vol. 21, no. 4, pp. 192–199, Apr. 2006.

[10] R. J. Klee and T. E. Graedel, "ELEMENTAL CYCLES: A Status Report on Human or Natural Dominance," *Annual Review of Environment and Resources*, vol. 29, no. 1, pp. 69–107, Nov. 2004.

[11] R. B. Herbert, S. G. Benner, and D. W. Blowes, "Solid phase iron–sulfur geochemistry of a reactive barrier for treatment of mine drainage," *Applied Geochemistry*, vol. 15, no. 9, pp. 1331–1343, Oct. 2000.

[12] K. G. Taylor and K. O. Konhauser, "Iron in Earth Surface Systems: A Major Player in Chemical and Biological Processes," *Elements*, vol. 7, no. 2, pp. 83–88, Apr. 2011.

[13] S. J. Brown, W. N. Goetzmann, and J. Park, "Careers and Survival: Competition and Risk in the Hedge Fund and CTA Industry," *The Journal of Finance*, vol. 56, no. 5, pp. 1869–1886, Oct. 2001.

[14] R. M. Cornell and U. Schwertmann, *The Iron Oxides*. Weinheim, FRG: Wiley-VCH Verlag GmbH & Co. KGaA, 2003.

[15] H. B. Bradl, "Adsorption of heavy metal ions on soils and soils constituents," *Journal of Colloid and Interface Science*, vol. 277, no. 1, pp. 1–18, Sep. 2004.

[16] F. M. G. Tack, E. Van Ranst, C. Lievens, and R. E. Vandenberghe, "Soil solution Cd, Cu and Zn concentrations as affected by short-time drying or wetting: The role of hydrous oxides of Fe and Mn," *Geoderma*, vol. 137, no. 1–2, pp. 83–89, Dec. 2006.

[17] G. A. Parks, "The Isoelectric Points of Solid Oxides, Solid Hydroxides, and Aqueous Hydroxo Complex Systems," *Chemical Reviews*, vol. 65, no. 2, pp. 177–198, Apr. 1965.

[18] D. A. Sverjensky, “Zero-point-of-charge prediction from crystal chemistry and solvation theory,” *Geochimica et Cosmochimica Acta*, vol. 58, no. 14, pp. 3123–3129, Jul. 1994.

[19] V. Chatain *et al.*, “Mineralogical study and leaching behavior of a stabilized harbor sediment with hydraulic binder,” *Environmental Science and Pollution Research*, vol. 20, no. 1, pp. 51–59, Jan. 2013.

[20] B. Kim, M. Gautier, C. Rivard, C. Sanglar, P. Michel, and R. Gourdon, “Effect of Aging on Phosphorus Speciation in Surface Deposit of a Vertical Flow Constructed Wetland,” *Environmental Science & Technology*, vol. 49, no. 8, pp. 4903–4910, Apr. 2015.

[21] B. Kim *et al.*, “pH and Eh effects on phosphorus fate in constructed wetland’s sludge surface deposit,” *Journal of Environmental Management*, vol. 183, pp. 175–181, Dec. 2016.

[22] J. Couvidat, V. Chatain, H. Bouzahzah, and M. Benzaazoua, “Characterization of how contaminants arise in a dredged marine sediment and analysis of the effect of natural weathering,” *Science of The Total Environment*, vol. 624, pp. 323–332, May 2018.

[23] A. El-Mufleh *et al.*, “Review on physical and chemical characterizations of contaminated sediments from urban stormwater infiltration basins within the framework of the French observatory for urban hydrology (SOERE URBIS),” *Environmental Science and Pollution Research*, vol. 21, no. 8, pp. 5329–5346, Apr. 2014.

[24] H. Bouzahzah, A. Califice, M. Benzaazoua, R. Mermillod-Blondin, and E. Pirard, “Modal Analysis of Mineral Blends Using Optical Image Analysis Versus X-Ray Diffraction,” p. 8, 2008.

[25] F. Zeng *et al.*, “The influence of pH and organic matter content in paddy soil on heavy metal availability and their uptake by rice plants,” *Environmental Pollution*, vol. 159, no. 1, pp. 84–91, Jan. 2011.

[26] I. G. Edeh, C. A. Igwe, P. I. Ezeaku, and University of Nigeria, “EFFECTS OF RUMEN DIGESTA ON THE PHYSICO-CHEMICAL PROPERTIES OF SOILS IN NSUKKA, SOUTHEASTERN NIGERIA,” *Russian Journal of Agricultural and Socio-Economic Sciences*, vol. 40, no. 4, pp. 3–11, Apr. 2015.

[27] M. Kumar *et al.*, “Variable Lime Requirement Based on Differences in Organic Matter Content of Iso-acidic Soils,” vol. 25, no. 1, p. 6, 2012.

[28] D. Goutaland *et al.*, “Hydrostratigraphic Characterization of Glaciofluvial Deposits Underlying an Infiltration Basin Using Ground Penetrating Radar,” *Vadose Zone Journal*, vol. 7, no. 1, p. 194, 2008.

[29] S. W. Poulton and D. E. Canfield, “Development of a sequential extraction procedure for iron: implications for iron partitioning in continentally derived particulates,” *Chemical Geology*, vol. 214, no. 3–4, pp. 209–221, Jan. 2005.

[30] N. L. Creeper, W. S. Hicks, P. Shand, and R. W. Fitzpatrick, “Geochemical processes following freshwater reflooding of acidified inland acid sulfate soils: An in situ mesocosm experiment,” *Chemical Geology*, vol. 411, pp. 200–214, Sep. 2015.

[31] T. Sukitprapanon, A. Suddhiprakarn, I. Kheoruenromne, S. Anusontpornperm, and R. J. Gilkes, “A comparison of potential, active and post-active acid sulfate soils in Thailand,” *Geoderma Regional*, vol. 7, no. 3, pp. 346–356, Sep. 2016.

[32] T. Sukitprapanon, A. Suddhiprakarn, I. Kheoruenromne, and R. J. Gilkes, “Partitioning and potential mobilization of aluminum, arsenic, iron, and heavy metals in tropical active and post-active acid sulfate soils: Influence of long-term paddy rice cultivation,” *Chemosphere*, vol. 197, pp. 691–702, Apr. 2018.

[33] S. R. Claff, L. A. Sullivan, E. D. Burton, and R. T. Bush, “A sequential extraction procedure for acid sulfate soils: Partitioning of iron,” *Geoderma*, vol. 155, no. 3–4, pp. 224–230, Mar. 2010.

[34] P. M. V. Bodegom and J. V. Reeven, “Prediction of reducible soil iron content from iron extraction data,” p. 16.

[35] Q. Huang *et al.*, “Influence of rice cultivation on the abundance and fractionation of Fe, Mn, Zn, Cu, and Al in acid sulfate paddy soils in the Pearl River Delta,” *Chemical Geology*, vol. 448, pp. 93–99, Jan. 2017.

[36] T. Winiarski, “FONCTION FILTRATION D’UN OUVRAGE URBAIN - CONSEQUENCE SUR LA FORMATION D’UN ANTHROPOSOL,” p. 199.

[37] M. Sáez, “A comparative study of the adsorption of linear alkylbenzene sulfonates and their biodegradation intermediates on marine sediments and organisms,” *Ciencias Marinas*, vol. 29, no. 4, pp. 397–403, Aug. 2003.

[38] S. E. Agarry and C. N. Owabor, “Anaerobic bioremediation of marine sediment artificially contaminated with anthracene and naphthalene,” *Environmental Technology*, vol. 32, no. 12, pp. 1375–1381, Sep. 2011.

[39] AFNOR, 2005. Recueil Normes et Réglementations Environnement. Qualité de l’eau. Vol 1 et 2. (Standard Collection and Regulatory Environment. Water Quality).

[40] Arrêté ministériel NOR: DEVO0650505A du 9 août 2006 relatif aux niveaux à prendre en compte lors d'une analyse de rejets dans les eaux de surface ou de sédiments marins, estuariens ou extraits de cours d'eau ou canaux. https://www.legifrance.gouv.fr/affichTexte.do?cidTexte=JORFTEXT000000423497, Accessed 22 May 2019.